ANALYSING INTERLACING PATTERNS IN 3D CARBON FIBRE REINFORCEMENTS

Salekrostam, R[1]*, Muzar, D[1] and Robitaille, F[1]
[1] Department of Mechanical Engineering,
University of Ottawa, Ottawa, Canada
* Corresponding author (rsale051@uottawa.ca)

Keywords: *Interlacing, 3D reinforcements, Carbon fibre preforms*

ABSTRACT

Carbon fibre polymer matrix composites (CF-PMC) are used in numerous applications including aerospace, infrastructure, defence, chemical industries and sporting goods. Traditional fabrics used as reinforcements for textile composites consist of thin weaves or stitched fabrics. This limits the performance of the composites in terms of resistance to impact and inter-laminar shear strength (ILSS), both leading to delamination. 3D reinforcements were introduced to mitigate and overcome these limitations. Many interlaced textile structures were developed but many more possibilities exist for yarn interlacing patterns, leading to different types of 3D textiles that may potentially be built. A limited number of 3D interlacing patterns are frequently referred to in the literature including orthogonal and interlock constructions, but little formal quantification of possible interlacing patterns is available. No algorithm describing all possible interlacing patterns in 3D textiles was published. Therefore, if one wishes to select or create a 3D textile reinforcement, no established formalism or language describing possible interlacing patterns exists, making productive discussion and comparison of interlacing patterns difficult. This work focuses on analysing 3D interlacing patterns which may be used in making 3D woven reinforcements. Criteria are established for selecting patterns that may be most favourable in view of their properties as reinforcements for CF-PMCs.

1 INTRODUCTION

3D textile reinforcements have seen increased use toward the fabrication of PMCs as composite parts made from such reinforcements offer better mechanical properties through the thickness compared with composite parts made from traditional 2D fabrics [1-4]. Better resistance to delamination and toughness constitute other advantages of composite parts made from 3D reinforcement compared with composite parts made from traditional 2D fabrics [5-8].

Interlacing patterns have a critical effect on resistance to delamination in composite parts, and also on the behaviour of dry textiles subjected to different loading cases [5]. Various physical properties of 3D textile reinforcements must be estimated or predicted for effective engineering of PMC manufacturing processes and composite part performance. Different reinforcement architectures and geometries are known to affect their various physical properties relating to processing and performance, say heat transfer properties, permeability and others. Therefore, the internal geometry and configuration of yarns in textile reinforcements should be probed based on a clear formalism describing it [9].

3D interlacing patterns were identified and quantified in previous work done by the authors, followed by elimination of similar interlacing patterns [10]. In this paper, different criteria are used for analysing and optimizing the behaviour of dry fabrics and composite parts.

2 ANALYSING 3D PREFORMS

2.1 UO-SPT preforming

The University of Ottawa Steered Preforming Technology (uO-SPT) enables the production of thick, flat, drapable final shape reinforcements by laying down individual yarns along the X and Y directions. The yarn lay-down sequence is entirely variable to create different interlacing patterns in the preforms. Yarns can be laid down along curvilinear paths with varying spacing. Both characteristics alter the behaviour of preforms in different loading cases such as compaction or in-plane shear [10, 11] and they change the mechanical properties of composite parts made from such fabrics consequently. The first characteristic is probed in this work.

Classic 3D interlacing patterns were identified in the literature and categorized in view of their internal structures. 3D angle interlock and 3D warp interlock interlacing patterns are examples of classic 3D interlacing patterns. Many more interlacing patterns may be created, which are not identified formally in the literature. Figure 1 shows different interlacing patterns for unit cells of the same size and featuring the same numbers of layers, which result in 6 different 3D textile reinforcements.

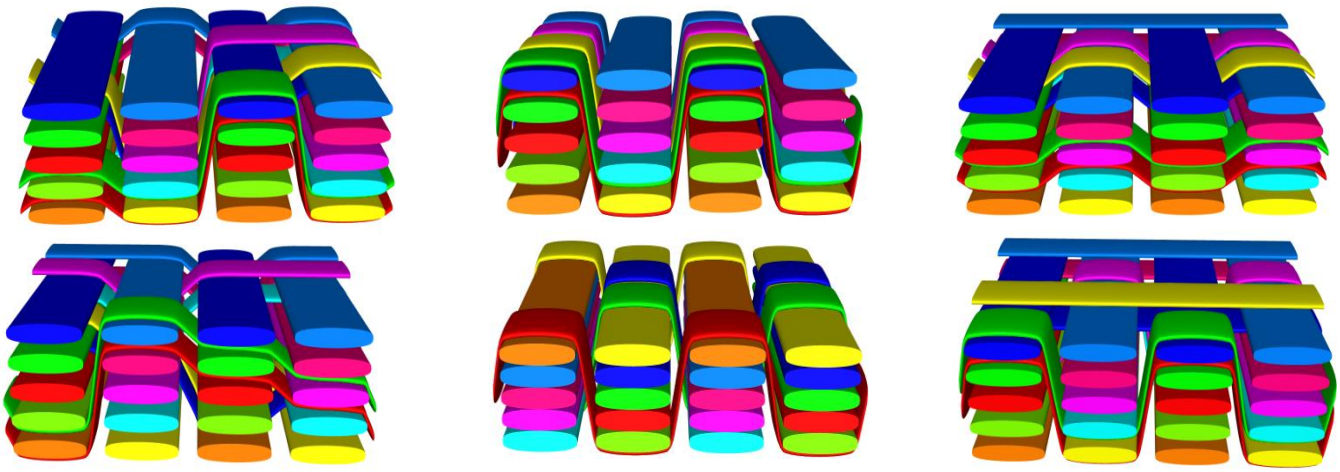

Figure 1: Different interlacing patterns resulting in different 3D textile reinforcements

2.2 Quantifying unique interlacing patterns

Analysing 3D interlacing patterns requires a capability for defining and quantifying all possible interlacing patterns that may be created. A formalism was developed for representing interlacing patterns as follows. Each yarn is identified by a layer integer corresponding to the layer to which the yarn belongs, from bottom to top. One sequence of layer integers is associated with each crossover in the textile unit cell, again from bottom to top; these sequences vary with interlacing. The number of possible sequences of layer integers at each crossover is finite, hence each possible sequence is identified by a sequence integer. The interlacing matrix representation consists of a matrix that features sequence integers for all crossovers in the unit cell. Therefore, each entry of the interlacing matrix represents the sequence of layer integers at a crossover. The number of possible sequences of yarns at each crossover depends on the number of layers. An integer from 0 to (L!-1) is assigned to each sequence. In a 2-layers, 2 by 2 unit cell featuring 4 yarns and 4 crossovers, each crossover can feature any of 2 different sequences. Each of the 4 integer entries in the interlacing matrix represents a sequence of 2 layer integers, in order of appearance from bottom to top. Figure 2 illustrates two different 2-layers, 2 by 2 unit cells and interlacing matrices.

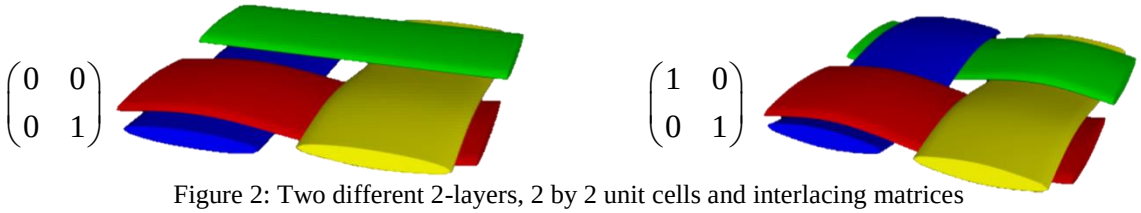

Figure 2: Two different 2-layers, 2 by 2 unit cells and interlacing matrices

The structure of a reinforcement textile is defined by its unit cell, which is its smallest repeated interlacing pattern. Here, rectangular unit cells feature N_X and N_Y available paths along X or Y respectively, along which layers of yarns will superimpose. The number IP of theoretically possible interlacing patterns is calculated as:

$$IP = (L!)^{N} \tag{1}$$

where L is the number of layers in the preform and N is the total number of crossovers with $N = N_X \times N_Y$. Some interlacing patterns generated in a first step are equivalent as they represent the same unit cell with applied rotations or translations relative to either X or Y. After quantifying the total number of possible interlacing patters, equivalent patterns are eliminated and the number of remaining interlacing patterns is termed total number of unique possible interlacing patterns, IP_e . Figure 3 illustrates four 6-layers, 4 by 4 unit cells that are equivalent by rotation around their centre.

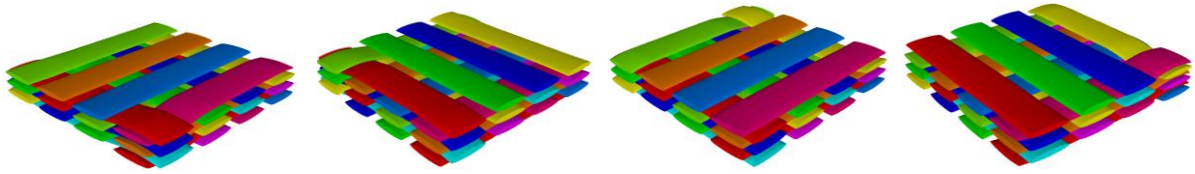

Figure 3: Equivalent 6-layers, 4 by 4 unit cells equivalent by rotation around their centre

2.3 Identifying and quantifying interlacing patterns that can be made using uO-SPT

The next step consists in eliminating interlacing patterns that cannot be made using the uO-SPT process, referred to as non-SPT interlacing patterns. Because of the nature of uO-SPT, yarns are laid down on top of each other individually in each direction, precluding unit cells that interlace as a weave does. This characteristic leads to the criterion for eliminating interlacing patterns that cannot be made using uO-SPT.

The criterion for identifying these interlacing patterns is applied on the sequences of layer integers at 4 crossovers in the unit cell, as follows. Each sequence integer in the interlacing matrix, which takes a value from 0 to (L!-1), is replaced by the corresponding sequence of layer integers. This results in a matrix with the same number of entries as the interlacing matrix, which is termed sequence matrix. Each entry of the sequence matrix is a vector of L integers, which is the sequence of layer integers. Figure 4 illustrates interlacing matrices and sequence matrices for a 3-layers 2 by 2 unit cell on the left and a 4-layers 3 by 3 unit cell on the right.

$$\begin{pmatrix} 0 & 1 \\ 0 & 1 \end{pmatrix} \equiv \begin{pmatrix} 1,2,3 & 1,3,2 \\ 1,2,3 & 1,3,2 \end{pmatrix} \qquad \begin{pmatrix} 0 & 2 & 1 \\ 2 & 6 & 0 \\ 1 & 8 & 0 \end{pmatrix} \equiv \begin{pmatrix} 1,2,3,4 & 1,3,2,4 & 1,2,4,3 \\ 1,3,2,4 & 2,1,3,4 & 1,2,3,4 \\ 1,2,4,3 & 2,3,1,4 & 1,2,3,4 \end{pmatrix}$$

Figure 4: Interlacing and sequence matrices for 3-layers 2 by 2 (left) and 4-layers 3 by 3 (right) unit cells

Identifying non-SPT textiles is best understood when illustrated using the sequence matrices. Any 4 crossovers located along any 2 columns and any 2 rows of the sequence matrix are considered; these 4 crossovers form the 4 corners of a rectangular clockwise loop. The even and odd layer integers along X and Y directions are compared. For a 4-layers textile, layer integers 1 and 3 are compared with layer integers 2 and 4, one by one. For example, the sequences 1,2 ; 3,2 ; 1,4 and 3,4 are compared in any loop in the sequence matrix. Along any rectangular loop, at least one of the sequences must appear twice at immediately neighbouring crossovers – not along diagonals – for the textile to be a SPT textile; for it to be made using uO-SPT. As an example, Figure 5 represents the interlacing matrix and sequence matrix of a 4-layers 2 by 2 unit-cell. The process of analysing the pattern shown in Figure 5 for feasibility using uO-SPT is illustrated in Figure 6. Figure 6a shows checks on layer integers 1 and 2. Each sequence appears twice at neighbouring crossovers in the sequence matrix, highlighted in blue and green. Inspection proceeds to the next steps that compares the following layer integers, Figures 6b, 6c, 6d. Sequences 2,3 and 1,4 appear everywhere, whilst sequence 3,4 appears in 3 immediately neighbouring positions. For each combination of layer numbers at least one sequence of the relevant integer layers appears in at least two neighbouring crossovers. The interlacing matrix of Figure 5 presents a textile that can be made using uO-SPT.

$$\begin{pmatrix} 0 & 0 \\ 7 & 6 \end{pmatrix} \equiv \begin{pmatrix} 1,2,3,4 & 1,2,3,4 \\ 2,1,4,3 & 2,1,3,4 \end{pmatrix}$$

Figure 5: 4-layers 2 by 2 interlacing matrix and substitute matrix

a $\begin{pmatrix} 1,2,3,4 & 1,2,3,4 \\ 2,1,4,3 & 2,1,3,4 \end{pmatrix}$ b $\begin{pmatrix} 1,2,3,4 & 1,2,3,4 \\ 2,1,4,3 & 2,1,3,4 \end{pmatrix}$ c $\begin{pmatrix} 1,2,3,4 & 1,2,3,4 \\ 2,1,4,3 & 2,1,3,4 \end{pmatrix}$ d $\begin{pmatrix} 1,2,3,4 & 1,2,3,4 \\ 2,1,4,3 & 2,1,3,4 \end{pmatrix}$

Figure 6: Analysing a 4-layers 2 by 2 textile for SPT process

Figure 7 shows a non-SPT 2-layers 3 by 3 unit cell, its interlacing matrix representation and its sequence matrix. The red highlight identifies 4 crossovers forming a loop where no crossover has any two identical layer integers in the sequence matrix. This confirms that the interlacing pattern cannot be made using uO-SPT. The list of IP_u unique possible interlacing patterns that can be made using uO-SPT is generated by eliminating all non-SPT interlacing patterns from IP_e. Table 1 shows IP, IP_e and IP_u for the case of a 3-layers, 2 by 2 unit cell.

Unit cell	No. of crossovers N	No. of layers L	IP	IP_e	Remaining (%)	IP_u	Remaining (%)
3-layers, 2×2	4	3	1296	231	17.8	29	2.2

Table 1: List of possible interlacing patterns before and after eliminations

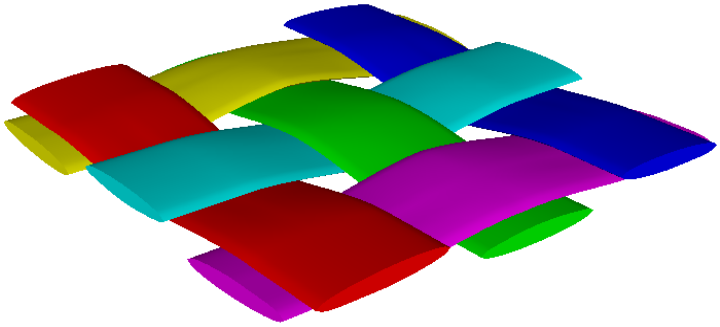

$$\begin{pmatrix} 0 & 1 & 0 \\ 1 & 0 & 1 \\ 0 & 1 & 0 \end{pmatrix} \equiv \begin{pmatrix} 1,2 & 2,1 & 1,2 \\ 2,1 & 1,2 & 2,1 \\ 1,2 & 2,1 & 1,2 \end{pmatrix}$$

Figure 7: 2-layers 3 by 3 non-SPT unit cell, interlacing matrix and sequence matrix

2.4 Criteria applicable to unit cells

The next step consists in defining criteria for analysing different interlacing patterns of 3D textile unit cells. Criterion 1 is the total interlacing index for yarns extending along X, I_{TX}. This criterion quantifies the total amount of interlacing for yarns extending along X, normalized by the total number of yarns extending along X, T_X and the number of paths along Y, N_Y, as presented in Equation 2:

$$I_{TX} = \frac{\sum_{X=0}^{T_X} I_X}{T_X * N_Y} \tag{2}$$

Associated criterion 2 is the total interlacing index for yarns along Y, I_{TY}. This criterion quantifies the total amount of interlacing for yarns extending along Y, normalized by T_Y and N_X as presented in Equation 3:

$$I_{TY} = \frac{\sum_{Y=0}^{T_Y} I_Y}{T_Y * N_X} \tag{3}$$

where T_Y is the total number of yarns extending along Y and N_X is the number of available paths along X. I_X and I_Y are determined by summing the absolute values of differences in sequences of layer integers in the sequence matrix, from one crossover to the next, for each yarn extending along X and Y. In Figure 8, I_X is 4 for yarn #1, 2 for yarn #2 and 0 for yarn #3.

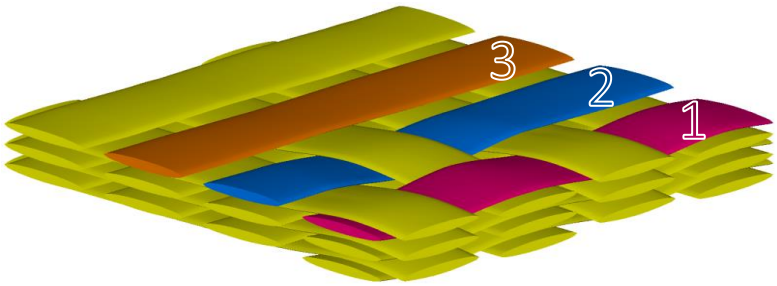

Figure 8: Interlacing index I_X for three yarns in a unit cell

Figures 9 and 10 show I_{TX} and I_{TY} values for different 4-layers 3 by 3 unit-cells with dissimilar interlacing patterns.

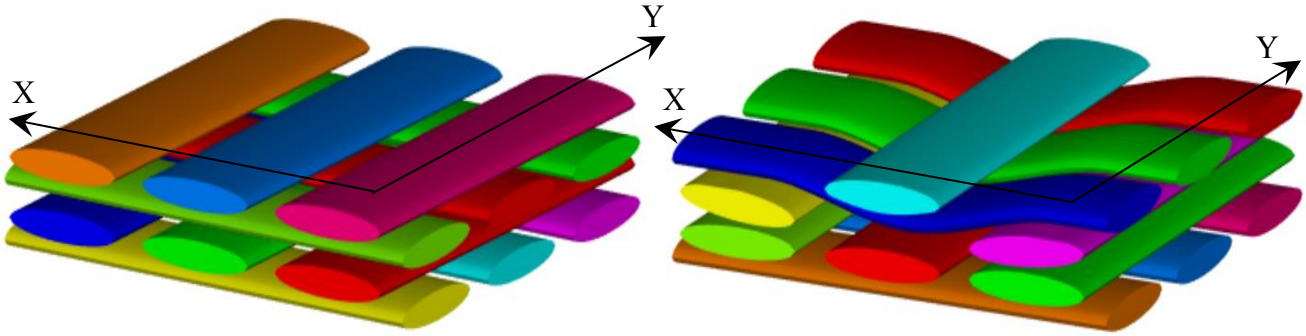

$I_{TX} = 0$, $I_{TY} = 0$ $\qquad$ $I_{TX} = \frac{6}{(6*3)} = 0.33$, $I_{TY} = 0$

Figure 9: 4-layers, 3 by 3 unit cells with different I_{TX} values

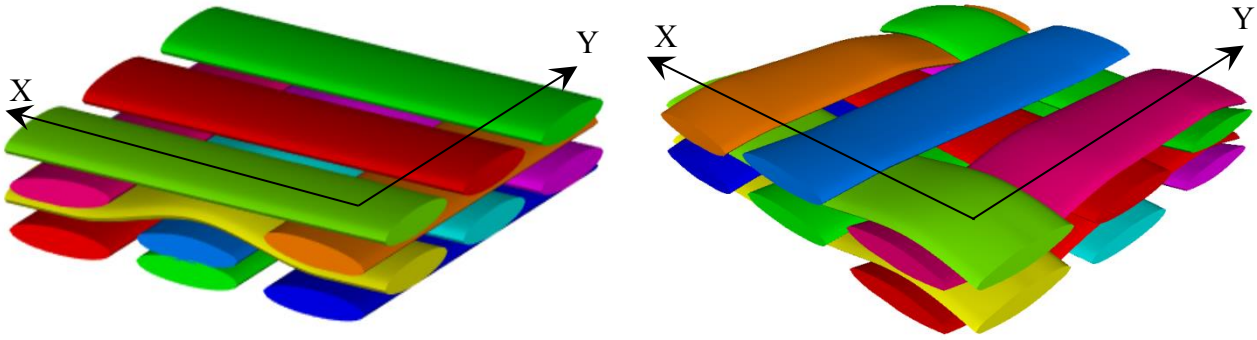

$I_{TX} = \frac{6}{(6*3)} = 0.33$, $I_{TY} = 0$ $I_{TX} = \frac{8}{(6*3)} = 0.45$, $I_{TY} = \frac{8}{(6*3)} = 0.45$

Figure 10: 4-layers, 3 by 3 unit cells with different I_{TX} and I_{TY} values

Criterion 3 is the crimp factor matrix **[C_{fi}]**. This criterion quantifies the distribution of crimp in the plane of the unit cell; it also illustrates which crossovers host higher crimp. The crimp factor matrix has the same dimensions as the interlacing matrix. Its entries C_{f1}, C_{f2}… C_{fN} are labelled crimp factors. Crimp factor C_{fi} of crossover index i is the maximum crimp of all yarns passing through this crossover. It is calculated by normalizing the maximum interlacing index of all yarns passing through the crossover, labelled $I_{c\text{-}max}$, by the number of layers L as presented in Equation 4:

$$C_f = \frac{I_{c-max}}{L} \tag{4}$$

where $I_{c\text{-}max}$ at each crossover is calculated using Equation 5:

$$I_{c-max} = Max(I_X, I_Y) \tag{5}$$

Figure 11 shows a generic crimp factor matrix for unit cells with $N_X = N_Y = 3$. It should be noted that the size of the crimp factor matrix does not depend on the number of layers in the textile.

$$\begin{pmatrix} C_{f1} & C_{f2} & C_{f3} \\ C_{f4} & C_{f5} & C_{f6} \\ C_{f7} & C_{f8} & C_{f9} \end{pmatrix}$$

Figure 11: Crimp factor matrix for unit cells with 9 crossovers

Figure 12 compares 3-layers, 3 by 3 unit-cells in terms of crimp distribution. The crimp factor matrix of Figure 12a shows an even distribution of crimp while in Figure 12b, the maximum crimp indexes are 0 in crossovers 1 through 6 and 0.67 in crossovers 7 through 9. Comparing the crimp factor matrices shows that the unit-cells of figure 12b and 12c have similar crimp factor matrix. This can be confirmed by the fact that these two unit-cells are equivalent by translation.

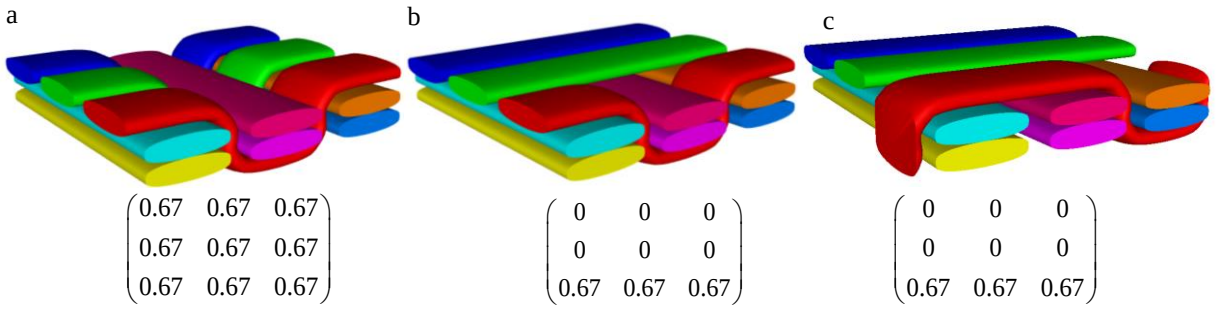

Figure 12: Comparing distribution of crimp in three different 3-layers 3 by 3 unit cells

The crimp factor matrix can also be used for comparing different textiles in terms of maximum crimp value. Figure 13 presents three different 3-layers, 3 by 3 unit-cells and their crimp factor matrices. Figure 13a features no interlacing hence the level of crimp in all 9 crossovers is 0. Figures 13b and 13c illustrate different levels of crimp in the unit-cells; this also appears in the crimp matrices.

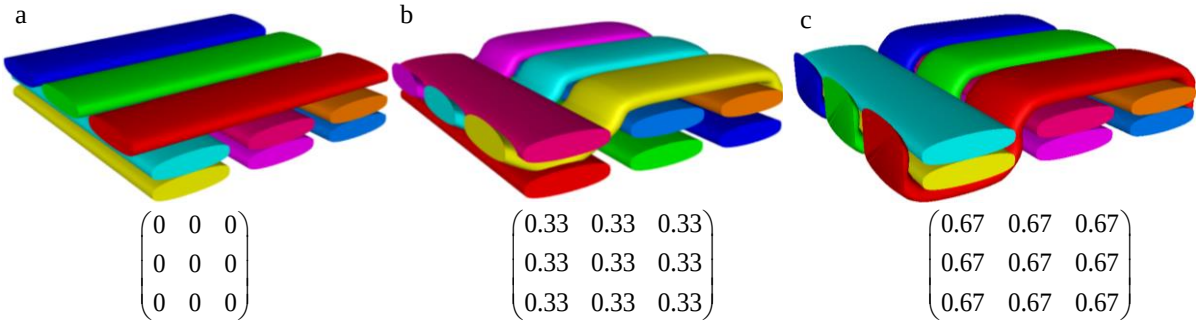

Figure 13: Comparing level of crimp in 3-layers 3 by 3 unit cells

2.5 Textile Analysis

The above criteria can be used for analysing 3D textiles through their interlacing patterns. IP_e patterns will be analysed in the case of classic 3D textile unit cells, and IP_u patterns will be analysed in the case of 3D textiles made using the uO-SPT process.

One challenge in forming dry 3D fabrics relates to their ability to bend around tight radii and cover curved surfaces without winkling. Figure 14 illustrates a 4-layers textile before and after bending for the basic case of a single curvature surface of constant radius. Whilst the same length L_1 can be associated with all layers before the textile is bent (left), different nominal lengths will be associated with different layers afterwards as a function of the radius (right). In a first analysis, yarns extending parallel to the axis of curvature and parallel to each other may be separated or brought closer to each other upon bending, with limited foreseeable consequences other than changes in local fibre volume fraction v_f. As for yarns extending perpendicular to the axis of curvature, hence undergoing actual bending, it is generally accepted that if compressive displacements are applied to these yarns they will buckle with detrimental consequences to the textile and eventual composite. On the other hand, these stiff yarns will not extend upon bending but they may adapt to larger radii by straightening and pulling into the textile and closer to the centre of curvature, hence deviating from their

nominal curve. Alternatively, the presence of interlacing and crimp in yarns located on outer radii may enable easier adapting of yarns to the curvature.

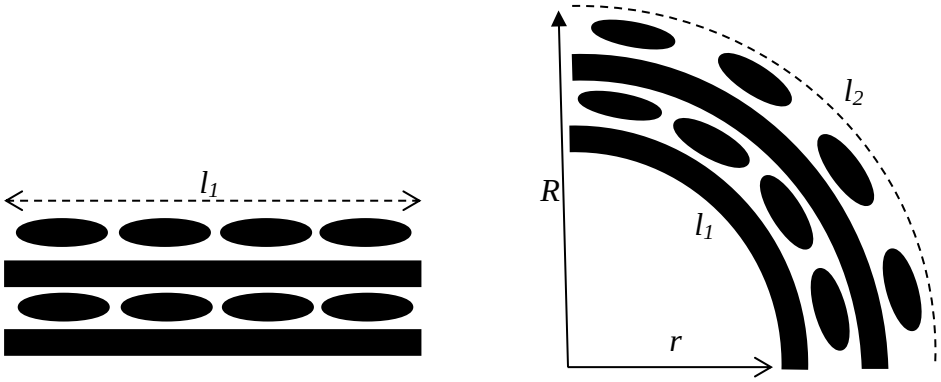

Figure 14: Diagram of 4-layer dry textile devoid of interlacing, before and after bending

Textiles and interlacing patterns may be designed to compensate the increase in nominal length from l_1 to l_2 due to the bending process. The difference in length between l_2 and l_1 is calculated as:

$$l_1 = \frac{\pi r}{2} \tag{6}$$

$$l_2 = \frac{\pi R}{2} = \frac{\pi (r + Lt)}{2} \tag{7}$$

$$l_2 - l_1 = \frac{\pi (r + Lt)}{2} - \frac{\pi r}{2} = 1.57Lt \tag{8}$$

where L is the number of layers in which the length is calculated and t is the nominal thickness of a layer of yarns.

The above equations apply to the frequent case of bends around a 90º single-curvature corner; they can easily be adapted to other angles but more to the point, they are useful in defining criteria and analysing bending for different interlacing patterns. The number of unit cells going around a corner is immaterial; for the nominal case, only the ratios of radii to thickness have an impact on the bending behaviour.

Reinforcement 3D textiles should be enable the extension of $1.57Lt$ in nominal path lengths. In a first, simplified analysis where the precise curvature and paths of yarns is disregarded, each occurrence of interlacing quantified by the normalized index I_{TX} nominally adds $2t$ to the length of the relevant yarn. The increase in nominal length of the interlaced yarn $2t \times I_{TX}$ is labelled L_3 and calculated as:

$$l_3 = l_1 + (2t \times I_{TX}) \tag{9}$$

Figure 15 shows an example of initial (left) and increased (right) lengths for a given yarn. In this case, length is increased by $8t$ which corresponds to an interlacing index of 4.

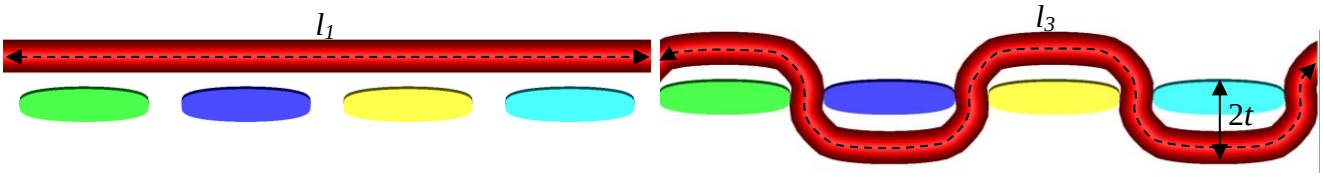

Figure 15: Initial yarn length l_1 (left) and interlaced yarn length l_3 (right)

Multi-layered textiles may better cover single-curvature surfaces without winkling if Equation 10 is satisfied. In this case, yarn length parallel to the axis of curvature suffices to extend in bending and cover the curved surface without creating buckling in the yarns and/or winkles in the textile.

$$l_3 - l_1 \geq l_2 - l_1 \tag{10}$$

Equations 8 and 9 are developed into Equations 11 and 12. Equation 12 provides a minimum value for the total interlacing index. 3D textiles can feature any interlacing pattern that satisfies the condition. It should be noted that in Equations 9, 11 and 12 the total interlacing index is calculated for the direction perpendicular to the axis of curvature. Equations are shown for cases where the axis of curvature is Y; if the axis of curvature is X, then I_{TX} should be replaced by I_{TY} in Equations 9, 11 and 12.

$$2t \times I_{TX} \geq 1.57Lt \tag{11}$$

$$I_{TX} \geq 0.785L \tag{12}$$

Another essential characteristic of 3D textiles is the stiffness in bending that will result in the final composite parts made from them. Crimp in yarns brings a knockdown factor to composite parts in terms of their stiffness. Composites featuring yarns that tend to be straight on outer layers will have better stiffness in bending; conversely, impact and inter-laminar behaviour may be best enhanced by creating interlacing closer to the mid-plane of the fabric where shear stresses under bending are maximized. Unit-cells with straight yarns at the outer layers are chosen, which means that $I_{TX\ (1,\ 2)} = 0$ and $I_{TX\ (L\text{-}1,\ L)} = 0$ where $I_{TX\ (1,\ 2)}$ and $I_{TX\ (L\text{-}1,\ L)}$ represent the interlacing index between first and second layer from bottom and top of the textile, respectively.

Improving the inter-laminar shear strength (ILSS) for the composite parts made from 3D textiles is an major goal in developing such textiles. In order to improve ILSS in composites the reinforcement should feature yarns extending through the thickness of the textile, and especially so at the mid-plane. This can be quantified using the crimp factor matrix. Entries of such matrix should have their maximum possible value as determined by Equation 14:

$$C_{f1} = C_{f2} = \ldots = C_{f9} = \frac{L-1}{L} \tag{14}$$

2.6 Selecting favourable interlacing patterns

Based on criteria including those listed above and the supporting equations, favourable interlacing patterns may be selected. As an example, different interlacing patterns for 4-layers, 3 by 3 unit-cells are analysed. Selected interlacing patterns are as follows.

Favourable bending behaviour of textiles with the axis of curvature extending along Y may be obtained with selected favourable unit-cell interlacing patterns listed as follows:

$$\begin{pmatrix} 1 & 0 & 1 \\ 1 & 0 & 1 \\ 1 & 0 & 1 \end{pmatrix}, \begin{pmatrix} 6 & 7 & 6 \\ 6 & 7 & 6 \\ 6 & 7 & 6 \end{pmatrix}$$

Favourable bending stiffness in composites may be obtained with selected unit-cell interlacing patterns as follows:

$$\begin{pmatrix} 0 & 2 & 0 \\ 0 & 2 & 0 \\ 0 & 2 & 0 \end{pmatrix}$$

Interlacing patterns that feature straight yarns at the outer surfaces of the 3D textile and different levels of interlacing at the mid-plane may be obtained with selected unit-cell interlacing patterns as follows:

$$\begin{pmatrix} 2 & 10 & 2 \\ 2 & 10 & 2 \\ 2 & 10 & 2 \end{pmatrix}$$

In this case, the crimp factor matrix is:

$$C_{fi} = \begin{pmatrix} 0.75 & 0.75 & 0.75 \\ 0.75 & 0.75 & 0.75 \\ 0.75 & 0.75 & 0.75 \end{pmatrix}$$

Figure 16 illustrates cross-sections of unit cells for three different interlacing patterns chosen as favourable interlacing patterns in view of different characteristics, with their interlacing matrix.

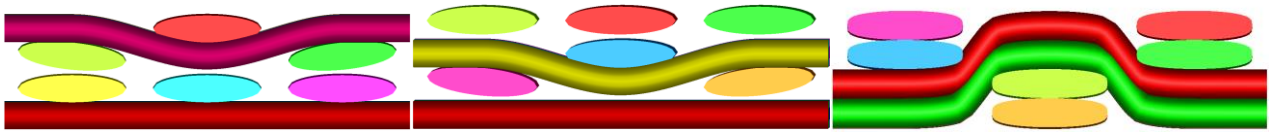

$$\begin{pmatrix} 1 & 0 & 1 \\ 1 & 0 & 1 \\ 1 & 0 & 1 \end{pmatrix} \quad \begin{pmatrix} 0 & 2 & 0 \\ 0 & 2 & 0 \\ 0 & 2 & 0 \end{pmatrix} \quad \begin{pmatrix} 2 & 10 & 2 \\ 2 & 10 & 2 \\ 2 & 10 & 2 \end{pmatrix}$$

Figure 16: Cross-sections of unit cells for three chosen interlacing patterns and their interlacing matrices

3 CONCLUSION

This paper focused on interlacing patterns for 3D textiles, which may be used as reinforcement in carbon fibre polymer matrix composites (CF-PMCs). All interlacing patterns that may be created upon manufacturing 3D reinforcements are identified. Then, equivalent/redundant interlacing patterns are identified and removed to generate a list of possible unique interlacing patterns featuring IP_e entries. Criteria are defined for identifying non-SPT interlacing patterns. Depending on the nature of the 3D textile being analysed, such interlacing patterns are quantified and removed from the list of possible unique interlacing patterns to generate the list of total possible SPT interlacing patterns featuring IP_u entries.

Criteria are defined towards enabling the ranking and analysis of the different interlacing patterns that may be created in 3D textile unit cells. The behaviour of 3D dry textiles and composite parts made from them can be probed in a first analysis through criteria such as those listed in the papers and others being developed. The aim is to offer means of querying likely behaviour of the dry reinforcement in bending upon forming for example, as well as the likely behaviour of the resulting composite in terms of bending stiffness or ILSS for example. Preferable interlacing patterns may be recommended from complete lists of those that may be produced, depending on requirements imposed by the manufacturing process of the fabric and loading case applied on the part.

4 REFERENCES

[1] J. Quinn, R. McIlhagger and A.T. McIlhagger. A modified system for design and analysis of 3D woven preforms. *Composites Part A: Applied Science and Manufacturing*, pp 503-509, 2003.

[2] D.S. Jetavat and P. Potluri. Extension of 3D weaving concepts for near-net preforming. *Proceeding of Structural Dynamics and Materials conference*, Schaumburg, IL, USA, 2008

[3] X. Chen and A.E. Tayyar. Engineering, manufacturing, and measuring 3D domed woven fabrics. *Textile Research Journal*, pp 375-380, 2003.

[4] M. McClain, J. Goering. Overview of Recent Developments in 3D Structures. *Albany Engineered Composites*, 2015.

[5] K. Wappat. HYBRIDMAT 4: Advances in the manufacture of 3-D preform reinforcement for advanced structural composites in aerospace. *Report of a DTI global watch mission, U. Department of Trade and Industry*, 2006.

[6] C.H. Chiu and C.C. Cheng. Weaving Method of 3D Woven Preforms for Advanced Composite Materials. *Textile Res*, pp 37-41, 2003.

[7] K. Fukuta and E. Aoki. 3D fabrics for structural composites. *Proceedings of the 15th Textile Research Symposium*, Philadelphia, 1986.

[8] X. Chen . Technical aspect: 3D woven architectures. *Proceedings of the NW TexNet*, Blackburn, 2007.

[9] N. Burnford. Development of drape simulation software and the optimization of variable-length textiles. *PhD thesis*, University of Ottawa, 2011.

[10] R.Salekrostam, D.Muzar and F.Robitaille. Interlacing patterns for steered yarn near net-shape 3D reinforcements. *SAMPE Conference Proceedings,* Seattle, WA, 2017.

[11] T. Divas. Manufacturing three-dimensional carbon-fibre preforms for aerospace composites. *MASc thesis*, University of Ottawa, 2014.